

**Plutonium interaction studies with the Mont Terri Opalinus Clay isolate Sporomusa sp. MT-2.99: changes in the plutonium speciation by solvent extractions.**

Moll, H.; Cherkouk, A.; Bok, F.; Bernhard, G.;

Originally published:

April 2017

**Environmental Science and Pollution Research 24(2017)15, 13497-13508**

DOI: <https://doi.org/10.1007/s11356-017-8969-6>

Perma-Link to Publication Repository of HZDR:

<https://www.hzdr.de/publications/Publ-24118>

Release of the secondary publication  
on the basis of the German Copyright Law § 38 Section 4.

# Plutonium interaction studies with the Mont Terri Opalinus Clay isolate *Sporomusa* sp. MT-2.99: changes in the plutonium speciation by solvent extractions

Henry Moll\*, Andrea Cherkouk, Frank Bok, and Gert Bernhard

Helmholtz-Zentrum Dresden-Rossendorf HZDR, Institute of Resource Ecology, Bautzner Landstrasse  
400, 01328 Dresden, Germany

## Abstract

Since plutonium could be released from nuclear waste disposal sites, the exploration of the complex interaction processes between plutonium and bacteria is necessary for an improved understanding of the fate of plutonium in the vicinity of such a nuclear waste disposal site. In this basic study the interaction of plutonium with cells of the bacterium, *Sporomusa* sp. MT-2.99, isolated from Mont Terri Opalinus Clay, was investigated anaerobically (in 0.1 M NaClO<sub>4</sub>) with or without adding Na-pyruvate as an electron donor. The cells displayed a strong pH dependent affinity for Pu. In the absence of Na-pyruvate a strong enrichment of stable Pu(V) in the supernatants was discovered, whereas Pu(IV)-polymers dominated the Pu oxidation state distribution on the biomass at pH 6.1. A pH-dependent enrichment of the lower Pu oxidation states (e.g. Pu(III) at pH 6.1 which is considered to be more mobile than Pu(IV) formed at pH 4) was observed in the presence of up to 10 mM Na-pyruvate. In all cases, the presence of bacterial cells enhanced removal of Pu from solution and accelerated Pu interaction reactions, e.g. biosorption and bioreduction.

**Keywords:** plutonium; bacteria; *Sporomusa* sp.; biosorption; bioreduction; solvent  
extractions

---

\* Address correspondence to Henry Moll, Institute of Resource Ecology, Helmholtz-Zentrum Dresden-Rossendorf HZDR, Bautzner Landstrasse 400, 01328 Dresden, Germany. E-mail: [h.moll@hzdr.de](mailto:h.moll@hzdr.de).

## Introduction

One potential source of actinides (An) in the environment could be the accidental release from nuclear waste disposal sites. Microorganisms indigenous in potential host rocks are able to influence the speciation and therefore the mobility of An and their retardation. They can as well affect the conditions in a geologic repository (e.g. by gas generation or canister corrosion). Currently salt, clay and granite are considered as potential host rocks for a nuclear waste disposal in Germany. Microorganisms are indigenous present in such subterranean environments and it was demonstrated that they can affect the speciation and hence the mobility of An in different ways (e.g. Lloyd and Gadd 2011; Swanson et al. 2012; Lütke et al. 2013; Wouters et al. 2013; Moll et al. 2014).

The impact of microbes and their secreted substances on the plutonium mobility and migration was highlighted in a recent review by Kersting (Kersting 2013). The need for a better mechanistic understanding for Pu at the molecular level to understand for instance its transport behaviour was pointed out. Plutonium as a redox sensitive element possesses a complicated chemistry because it can coexist in several oxidation states, i.e., +3, +4, +5 and +6, in aqueous solution under environmental conditions. Figure 1 depicts a generalized Eh – pH diagram that shows the dominant Pu species that exist for a range of Eh and pH values calculated under anaerobic conditions. Hence the mobility of plutonium depends on its speciation and is highly influenced by its oxidation state. The plutonium speciation can be affected by environmental bacteria in terms of ligand complexation, internal accumulation or uptake, external accumulation (e.g., biosorption), metal reduction and oxidation, and biomineralization through direct (enzymatic) (e.g. Kimber et al. 2012; Ohnuki et al. 2009 and 2010; Reed et al. 2007; Boukhalfa et al. 2007; Icopini et al. 2009) and indirect redox transformations (e.g. Neu et al. 2005; Lukšienė et al. 2012). Due to the diversity of microorganisms and the complexity of biogeochemical systems a wide range of bacterially mediated processes occurred (Neu et al. 2010; Newsome et al. 2014). For instance, the addition of citric acid and glucose to contaminated soil from the Nevada Test Site (NTS) stimulated indigenous microbial activity and enhanced the dissolution of Pu under aerobic and anaerobic conditions (Francis and Dodge 2015). The understanding of reactions between priority radionuclides such as Pu with microbes and on mineral surfaces is essential for the safe management of radioactive wastes in order to contribute to the remediation of radionuclide-contaminated land (Roh et al. 2015; Brookshaw et al. 2012). The sorption of Pu may involve adsorption of oxidized species including a combination of reduction and disproportionation reactions. Furthermore, Pu(V) and Pu(VI) can be reduced biotically to Pu(IV).

However, the role of complexing ligands in facilitating microbial reduction of Pu(VI) to Pu(III), and enhancing Pu(III) solubility is not well understood at present. At near-neutral pH residual organics, present in biologically active systems of *Shewanella alga* BrY, enzymatically reduce Pu(VI) to Pu(V) (Reed et al. 2007). Several aerobic and anaerobic bacteria (e.g. *Bacillus* sp., *Pseudomonas* sp., *Citrobacter* sp., and *Clostridium* sp.) were isolated from for instance leachate samples collected from for instance Pu contaminated soils (Francis 2007). Viable metabolically active microbes were detected at the Los Alamos (LANL), transuranic (TRU) waste burial site containing <sup>239</sup>Pu contaminated soil. A slight increase in microbial activity (respiration) can alter the redox potential and reduce Pu(VI) to Pu(V). Since the solubility of Pu(III) hydroxide is much greater a reduction of Pu(IV) oxyhydroxides to Pu(III) hydroxide is expected to increase the solubility of Pu in the environment. A reductive dissolution of Pu(IV) to Pu(III) by *Clostridium* sp. was observed (Francis et al. 2007 and 2008). Although Pu generally exists as insoluble Pu(IV) in the environment, under appropriate conditions, anaerobic microbial activity could affect the long-term stability and mobility of Pu by its reductive dissolution. The impact of the Fe(III)-reducing bacteria *Geobacter sulfurreducens* and *Shewanella oneidensis* MR-1 on the speciation of plutonium was investigated in (Renshaw et al. 2009). The results showed that in all cases, the presence of bacterial cells enhanced removal of Pu from solution. It could be demonstrated that the sorbed and precipitated Pu was mainly Pu(IV), but Pu(III) was also present. Hence, the microbial interactions with plutonium are complex and driven by a combination of initial sorption to the cell surface, followed by varying degrees of reduction, shown for Pu(VI) with *G. sulfurreducens* and for Pu(IV) with other bacteria studied. In our previous study, we investigated the interaction of plutonium in mixed oxidation states (Pu(VI) and Pu(IV)-polymers) with cells of the sulfate-reducing bacterial (SRB) strain *Desulfovibrio äspöensis* DSM 10631<sup>T</sup>, which frequently occurs in the deep granitic rock aquifers at the Äspö Hard Rock Laboratory (Äspö HRL), Sweden (Moll et al. 2006). At high initial Pu concentrations between 620 to 1033 µM and a dry biomass concentration of 1 g/L, the experiments showed that the cells could accumulate  $18 \pm 2$  mg Pu / g<sub>dry weight</sub> at pH 5. We used solvent extractions, UV-vis absorption spectroscopy and X-ray absorption near edge structure (XANES) spectroscopy to determine the speciation of Pu oxidation states. Extended X-ray absorption fine structure (EXAFS) spectroscopy was used to study the coordination of the Pu bound by the bacteria. In the first step, the Pu(VI) and Pu(IV)-polymers are bound to the biomass. Solvent extractions showed that 97 % of the initially present Pu(VI) is reduced to Pu(V) due to the activity of the cells within the first 24 h of contact time. Most of the formed

Pu(V) dissolves from the cell envelope back to the aqueous solution due to the weak complexing properties of this plutonium oxidation state.

The Opalinus Clay layer of the Mont Terri Underground Rock Laboratory (URL) is one potential host rock tested for nuclear waste disposal in Switzerland (Thury and Bossart 1999). The here investigated *Sporomusa* sp. MT-2.99 was recently isolated from Opalinus Clay core samples, collected from a borehole of the Mont Terri URL, Switzerland (Bachvarova et al. 2009). However, so far very little is known about the microbial activity in Mont Terri Opalinus Clay (Poulain et al. 2008) representing unfavorable living conditions as the lack of water and nutrients and small pores. Recently, indigenous bacteria from Mont Terri Opalinus Clay and its interactions with uranium, europium, and curium were investigated (Lütke et al. 2013; Moll et al. 2014). These studies demonstrated the ability of the two isolated strains *Sporomusa* sp. MT-2.99 and *Paenibacillus* sp. MT-2.2 to interact with An/Ln and hence to change whose speciation and migration characteristics.

In this study, research was focused on the unknown interaction of *Sporomusa* sp. MT-2.99 with plutonium. The accumulation of  $^{242}\text{Pu}$  by the bacteria was investigated in dependence on the contact time, the initial plutonium concentration,  $[\text{}^{242}\text{Pu}]_{\text{initial}}$ , within a pH range of 3 to 7 without and with adding Na-pyruvate as electron donor under strict anaerobic conditions due to the physiological needs of the studied bacterium. Solvent extractions and partly absorption spectroscopy were applied to explore the time dependent  $^{242}\text{Pu}$  oxidation state distribution a) in the blanks, b) the supernatants after separating from the cells and c) of the Pu bound on the bacteria.

## Materials and Methods

### Cultivation of bacteria

*Sporomusa* sp. MT-2.99 was isolated from the Mont Terri Opalinus Clay core samples collected from borehole BHT-1 from the Mont Terri URL, Switzerland (Bachvarova et al. 2009). For Pu interaction studies *Sporomusa* sp. MT-2.99 was grown under anaerobic conditions ( $\text{N}_2$  atmosphere) in liquid R2A medium (DSMZ medium 830) at 30°C. The cells were grown to the late exponential growth phase and harvested by centrifugation (8000xg). For plutonium interaction experiments under anaerobic conditions the cells were washed three times and re-suspended in degassed analytical grade 0.9 % NaCl (Sigma-

Aldrich, Germany) solution containing  $10^{-4}$  M Na-pyruvate (Sigma-Aldrich, Germany), respectively. The biomass of the cell stock suspension was determined by measuring the  $OD_{600}$ , which was then converted to the dry biomass according as described in Moll et al. 2014. The cell morphology and purity of the strain of each used cell stock suspension was examined as described elsewhere (Moll et al. 2014).

## Pu solution and quantification of Pu oxidation states by solvent extraction

The starting compound to obtain the  $^{242}\text{Pu}$  stock solution was a green-brown powder of  $\text{PuO}_2$  (AEA technology QSA GmbH) with the following composition: 0.009 % of Pu-238, 0.008 % Pu-239, 0.020 % Pu-240, 0.017 % Pu-241, 99.945 % Pu-242, and 0.001 % Pu-244. The problem is that this substance is chemically highly inert and dissolves extremely slowly in acids (Keller 1971). We performed an oxidative dissolution of  $^{242}\text{PuO}_2$  in  $\text{HNO}_3$  in the presence of  $\text{AgNO}_3$  and  $\text{K}_2\text{S}_2\text{O}_8$ . Finally the  $^{242}\text{Pu(VI)}$  stock solution in 3 M  $\text{HClO}_4$  was prepared by electrolysis. Because of the low absorption coefficients of Pu(IV), Pu(V), and Pu(IV)-polymers (Keller 1971; Wilson et al. 2005; Ockenden and Welch 1956) and the low concentration of Pu in the solutions, the quantification of the different Pu oxidation states was performed by solvent extraction by a procedure adapted from (Nitsche et al. 1988 and Nitsche et al. 1994) which was successfully applied in our previous study as described in (Moll et al. 2006). The extractions were performed rapidly and in parallel. The pH of the extraction samples was 0 or 1. Hence, the extraction procedure should not be affected by Pu hydrolysis. No hydrolysis dependence was reported in the original references (Nitsche et al. 1988 and Nitsche et al. 1994). From the LSC-measurements, we used the Pu-242 activity in each sample in order to calculate the fractions of the individual Pu oxidation states. Therefore, all fractions are given in activity %.

## Ultraviolet-visible-near infrared (UV-vis-NIR) absorption spectroscopy and liquid scintillation counting

Besides solvent extraction in selected samples the plutonium oxidation state distribution was checked by absorption spectroscopy in the ultraviolet-visible-near infrared (UV-vis-NIR) wavelength range. The absorption spectroscopy measurements were performed using a CARY5G UV-vis-NIR spectrometer (Varian Co.) at a temperature of  $22 \pm 1$  °C. All plutonium concentrations were measured by liquid scintillation counting (LSC) using a LS counter, Wallac system 1414 (Perkin Elmer). For this, defined

sample volumes (50 to 300  $\mu\text{L}$ ) were mixed with 5 mL of Ultima Gold scintillation cocktail (Sigma-Aldrich, Germany). The solvent extraction experiments demonstrated that the acidic Pu stock solution still contained, besides 73 % Pu(VI), 5 % Pu(III), and 19 % Pu(IV)-polymers due to the synthesis procedure.

## pH and redox potential measurements

The pH was measured using an InLab Solids electrode (Mettler-Toledo, Giessen, Germany) calibrated with standard buffers and a pH meter (Microprocessor pH Meter pH 537, WTW, Weinheim, Germany). The pH was adjusted with a precision of 0.05 units. The pH adjustments were made with  $\text{HClO}_4$  or NaOH both from Merck, Germany. The redox potential in blanks and cell suspensions was measured using a combination redox electrode (BlueLine 31 Rx from Schott, Germany) by applying the single point calibration using a redox buffer. The electrode was calibrated by measuring the potential in the redox buffer prior the Pu containing samples. The resulting error of the redox potentials was within 5 to 10 % of the given values. The error was derived from repeated measurements including small systematic drifts of the redox buffer.

## Pu-bacteria interaction experiments

The Pu-bacteria interaction experiments were performed at [dry biomass] of  $0.33 \pm 0.01 \text{ g}_{\text{dry weight}}/\text{L}$  and pH values of 3, 4, 6.1 and 7 under  $\text{N}_2$  atmosphere at 25 °C in 0.1 M  $\text{NaClO}_4$  solution.  $^{242}\text{Pu}$  initial was varied between 0.8 and 455  $\mu\text{M}$ . Na-pyruvate (Sigma-Aldrich, Germany), as one potential electron donor was added in two concentrations (0.1 and 10 mM) at pH 6.1. At pH 4 only one Na-pyruvate concentration (10 mM) was added. Samples were taken after defined time steps. The separation of cells from the supernatant solution was performed by centrifugation (6000xg). The  $^{242}\text{Pu}$  present in blank (no cells added), supernatant, and washed biomass suspension at pH 0 was analyzed using solvent extraction, and LSC as described above.

The adsorption of Pu onto the reaction vessel as source of error was investigated as well. Therefore, after the Pu interaction experiments the reaction tubes were rinsed 3 times with Milli-Q water and then incubated for 2 days with 1 M  $\text{HClO}_4$  to desorb Pu. Solutions were then analyzed with LSC regarding [Pu]. The determined loss of Pu was accounted for the calculation of the amount of Pu bound per g dry

biomass.

## Data analysis

The data evaluation was performed using the OriginPro 8.6G (OriginLab Corporation, USA) code. The time-dependent Pu concentrations measured in the supernatants were successfully fitted with bi-exponential decay functions. The time-dependent Pu oxidation state distributions were successfully fitted by using mono-exponential decay or growth functions.

## Results

### Accumulation of Plutonium ( $^{242}\text{Pu}$ ) by *Sporomusa* sp. as a function of pH

Our aim was to study the interaction process of Pu with *Sporomusa* sp. cells within a broad pH-range from the acidic up to the near-neutral pH region (pH 3, 4, 6.1, and 7). The pH of Mont Terri Opalinus Clay waters is expected to be in the neutral pH region (e.g. Joseph et al. 2013). A further reason for the chosen pH-range was to keep the investigations with Pu comparable with our previous studies of U(VI) interactions with the Mont Terri Opalinus Clay isolate *Paenibacillus* sp. (Lütke et al. 2013).

More Pu was removed by *Sporomusa* sp. MT-2.99 cells at pH 6.1 compared with the results measured at pH 4.0 especially in the absence of Na-pyruvate (cf. Figure 2 a and b). The time-dependent behavior of Pu in the supernatants was bi-exponential fitted ( $y = y_0 + A_1 e^{-(x/t_1)} + A_2 e^{-(x/t_2)}$ ). The kinetic fits showed that the overall process consists of at least two parts: a fast process having a time frame of  $\sim 0.5$  h (e.g., biosorption) and a much slower process with a time frame of  $\sim 1000$  h. At pH 4 and at initial Pu concentrations of 190 and 460  $\mu\text{M}$  (cf. Figure S1), it seems that *Sporomusa* has a slightly different strategy to avoid the stress caused by Pu compared with pH 6.1. For example at  $[\text{Pu}]_{\text{initial}}$  190  $\mu\text{M}$  after 2 h of contact time a strong decrease of the Pu concentration in solution was measured. The cells could release approximately 19 % of this bound Pu. It suggests that the cells could protect themselves for 24 h from the Pu. At incubation times  $\geq 24$  h an exponential decrease of the Pu concentration in solution was detected. This behavior was observed in all time-dependent experiments performed as a function of the initial Pu concentration.

The biosorption of Pu on *Sporomusa* sp. MT-2.99 cells was evaluated using the Langmuir absorption

isotherm model (cf. Figure 2c). The application of the Langmuir-isotherm model in order to describe the biosorption of heavy metals in biological systems (e.g. biosorption of heavy metals on algae) was reported for instance in (Klimmek 2003). At pH 6.1 the maximal Pu loading on *Sporomusa* sp. cells was calculated to be 230 mg Pu / g<sub>dry weight</sub> compared to 160 mg Pu / g<sub>dry weight</sub> at pH 4 (cf. Figure 2 c). The Langmuir constant b describes the affinity of the adsorbed metal to the bacterial surface (Kümmel and Worch 1990; Atkins 1998). The data showed that at pH 6.1 Pu has a 6 times higher affinity to the *Sporomusa* sp. MT-2.99 surface compared to pH 4. Panak and Nitsche (2001) reported that aerobic soil bacteria *B. sphaericus* and *P. stutzeri* accumulated between 30 and 75 mg Pu / g<sub>dry weight</sub> under comparable conditions at pH 5. This shows that *Sporomusa* sp. accumulated relatively high amounts of Pu. Additionally, *Sporomusa* sp. cells displayed a strong pH-dependent affinity for Pu (cf. Figure 2). At pH 3, only 13 % of the initial Pu was accumulated whereas at pH 7, 90 % were associated with the biomass (cf. Figure S2).

## Accumulation of Plutonium (<sup>242</sup>Pu) by *Sporomusa* sp. cells depending on addition of Na-pyruvate

Na-pyruvate was used as electron donor because characterization tests showed that this carbon source was best digested by the bacteria. The electron donor was used in the concentration range between 11 and 1100 mg/l. The total organic carbon (TOC) content of Mont Terri Opalinus Clay waters vary between 19 and 58 mg/l (Thury and Bossart 1999). The composition of the TOC is not known in detail at the moment.

At pH 4 the kinetic fits showed that the overall process consists of at least two parts: a fast process having a time frame of ~ 0.1 h (e.g., biosorption) and a much slower process with a time frame of ~ 120 h (cf. Figure S3a). We observed faster processes compared with the results when no Na-pyruvate was added. One reason for this observation could be the different Pu speciation and Pu redox chemistry in the presence of Na-pyruvate. At pH 6.1 the time-dependent decrease of Pu could be best fitted applying a mono-exponential decay law. This indicates one dominating step having a short time frame of 8.3 h (cf. Figure S3b).

A comparison of the cell bound Pu in dependence on pH and Na-pyruvate concentration was done with [Pu]<sub>initial</sub> of 57.8 µM. The accumulated amount of Pu was calculated based on the fit of the time-dependent Pu concentrations in the corresponding solution. At pH 4 in the absence of Na-pyruvate 24.4 ± 1.2 mg Pu / g<sub>dry weight</sub> was accumulated compared with 20.5 ± 0.7 mg Pu / g<sub>dry weight</sub> in the presence of 10

mM Na-pyruvate. At pH 6.1 the cells accumulated  $45 \pm 5$  mg Pu / g<sub>dry weight</sub> in pure 0.1 M NaClO<sub>4</sub>,  $42 \pm 6$  mg Pu / g<sub>dry weight</sub> in the presence of 0.1 mM Na-pyruvate, and only  $26 \pm 1$  mg Pu / g<sub>dry weight</sub> when 10 mM Na-pyruvate was present. The observed effect was highest at pH 6.1. Here, approximately half of the Pu amount was accumulated in the presence of 10 mM Na-pyruvate compared with the amount detected in the absence of Na-pyruvate. The observed differences in the bioassociation behavior of Pu might be related to the corresponding Pu speciation and redox chemistry in the presence and absence of Na-pyruvate. For example at pH 6.1 with 10 mM Na-pyruvate an increased amounts of Pu(III) (see next sections) were formed. This Pu(III) remained more mobile and hence was not associated on the biomass. Processes forming mobile Pu(III) in the presence of microbes were discussed in (e.g. Francis et al. 2007 and 2008, Boukhalfa et al. 2007). Up to present, we could not find any information of stability constants describing soluble Pu-pyruvate species. The lower tendency of bioassociation can be also explained by the formation of soluble Pu(III) (cf. Figure 3 C). Similar effects were observed by Boukhalfa et al. in their investigations with *G. metallireducens* GS-15 and *S. oneidensis* MR-1 (Boukhalfa et al. 2007).

## Reversibility of Pu bioassociation

To estimate the reversibility of the Pu bioassociation process, the Pu loaded biomasses were treated with 1 M HClO<sub>4</sub> in order to determine the amount of extractable Pu. In the absence of Na-pyruvate only 40 % of the plutonium was released at pH 6.1. In general, similar results were obtained at pH 4. These findings indicated that the interaction process is only partly reversible. Beside the formation of surface complexes with functional groups of the cell surface, and bio-reduction reactions other process can take place (e.g. emplacement in cell membrane structures). Also for Cm(III) and Eu(III) a certain amount (30 to 40 %) was identified to be irreversibly bound to the cells (Moll et al. 2014). At pH 4 in two samples the acidified biomasses were treated with 0.01 M EDTA at pH 5. In average  $31 \pm 3$  % of the strongly bound Pu could be released. Hence, 69 % of the irreversibly bound Pu remained on the biomass indicating a strong interaction with the cells. In contrast to the electron donor free experiments, we could measure that more than 80 % of the plutonium was released from the cells in the presence of 10 mM Na-pyruvate at pH 6.1. This might indicate a dominant complexation/fixation of plutonium on functional groups located at the cell surface. Desorption experiments were performed as a function of the pyruvate concentration. The average amounts of extractable Pu from the cells at [Pu]<sub>initial</sub> 58 µM were:  $41 \pm 7$  % no donor,  $55 \pm 11$  % 0.1 mM pyruvate, and  $93 \pm 3$  % 10 mM pyruvate. This showed that increased concentrations of pyruvate

increase also the contribution of a reversible surface complexation of Pu on the bacterial cell surface.

## Redox potential measurements

Under steady state conditions, at  $[Pu]_{\text{initial}}$  of 180  $\mu\text{M}$  in the biomass suspensions redox potentials of 800  $\pm$  40, 700  $\pm$  35, 425  $\pm$  21, and 535  $\pm$  27 mV were measured at pH 3, 4, 6.1, and 7, respectively (cf. Figure 1). In the blanks were always measured higher redox potentials of 1020  $\pm$  76, 1040  $\pm$  78, 790  $\pm$  75, and 870  $\pm$  65 mV, respectively at the corresponding pH values. Hence, the redox potential measurements indicated that the cells generated reducing conditions. The cell induced effect on the redox potential was highest at pH 6.1. Hence, the ability of the cells to decrease the redox potential depends on the pH. Concerning the time dependence at pH 6.1, in the blank sample at  $t \geq 312$  h a redox potential of 790  $\pm$  73 mV was measured. In the cell suspensions immediately a constant value of 424  $\pm$  21 mV was reached. The ability of the cells to reduce the redox potential in Pu containing cell suspensions depends also on the Pu concentration present. Because at pH 6.1 under steady state conditions and at  $[Pu]_{\text{initial}}$  62  $\mu\text{M}$  and 454  $\mu\text{M}$  the redox potential was measured to be 331 mV and 633 mV, respectively. The cell induced effect on the redox potential is smaller in the presence of 10 mM Na-pyruvate. Based on the redox potential measurements and besides abiotic reduction process of for instance Pu(VI) a cell induced effect on the time-dependent Pu oxidation state distribution is likely to occur and will be discussed in the following paragraph.

## Time-dependent Pu oxidation state distributions – no electron donor

*The blank.* In the beginning the dominating Pu species are Pu(VI), 58  $\pm$  7 %, Pu(IV)-polymers, 19  $\pm$  1 % and Pu(III), 13  $\pm$  6 % (see supplementary material Figure S4 a and b). The time-dependent behavior of Pu(VI) and Pu(V) was mono-exponential fitted ( $y = y_0 + A_1 e^{-(x/t_1)}$ ). The decrease of Pu(VI) at pH 6.1 is 3.2 times faster than at pH 4. The increase of Pu(V) at pH 6.1 is 3.3 times faster than at pH 4. At pH 6.1 and under steady state conditions the Pu(VI) amount decreased to 4  $\pm$  1 %, the Pu(V) amount increased to 76  $\pm$  4 % and the Pu(IV)-polymer amount was 13  $\pm$  4 %. The dominance of Pu(V) was also predicted in the Eh – pH calculations shown in Figure 1. Whereas at pH 4 under steady state conditions, higher amounts of Pu(VI) of 23.5  $\pm$  2 %, lower amounts of Pu(V) of 57  $\pm$  2 % were measured. The Eh – pH calculations predicted a dominance of Pu(VI) (cf. Figure 1). Here, the Pu(IV)-polymer amount remains constant at 19.6  $\pm$  0.8 % within the investigated time range. Concluding that a more acidic pH

stabilizes Pu(VI). This observation is in agreement with the Eh-pH calculations shown in Figure 1.

*The supernatant.* A significant change of the Pu oxidation state distributions was observed in the supernatants (cf. Figure 3 a and supplementary material Figure S4 c) compared with the blanks. At both pH values a fast decrease of Pu(VI) combined with a fast increase of Pu(V) was observed. At pH 6.1 the formation of Pu(V) in the supernatant is 48 times faster than in blank samples. Whereas the decrease of Pu(VI) in the supernatant is 28 times faster than in the blanks. The increase in the Pu(V) concentration is faster than expected. Because one should assume an equilibrium between the formation of Pu(V) and the decrease of Pu(VI) as observed in the blanks. One explanation could be the influence of the cells on the observed processes. At pH 6.1, the equilibrium concentration of Pu(V) in the supernatants is with ca. 90 % higher than in the blanks where 76 % was found. At pH 4 the formation of Pu(V) in the supernatant is 144 times faster than in blank samples. The decrease of Pu(VI) in the supernatant is 626 times faster than in the blanks. The decrease of Pu(VI) was much faster compared with the increase of Pu(V). Again, this discrepancy from equilibrium might be explained by the influence of the cells. The observed cell mediated reduction process of Pu(VI) to Pu(V) is not yet fully understood. After the interaction the majority of the Pu(V) was detected in solution (cf. Table 1). We assume that this happens due to the comparable weak complexing properties of the  $\text{PuO}_2^+$  ion which is related with a release from the cell envelope. Similar observations were made in the past (Panak and Nitsche 2001; Moll et al. 2006). The formed Pu(V) is relatively stable after removing the cells from solution. The dominance of Pu(V) in the supernatants/cell suspensions is also in agreement with the Eh-pH calculations shown in Figure 1 (for pH 3, 4, and 7). For the cell suspension at pH 6.1 predominantly Pu(IV) was predicted (cf. Figure 1). This could not be confirmed experimentally due to the dominance of Pu(V). At pH 6.1 the equilibrium concentration of the Pu(IV)-polymers was 6 % compared with 12.5 % found in the blanks. This suggests a pronounced biosorption of Pu(VI)-polymers on the biomass.

*UV-vis-NIR spectroscopy:* The time-dependent decrease of Pu(VI) (cf. Figure 4 a) and the increase of Pu(V) (cf. Figure 4 b) could be confirmed by UV-vis-NIR spectroscopy. The absorption band at 830 nm is associated with the  $\text{PuO}_2^{2+}$  ion (e.g. Cho et al. 2010). Red shifted absorption bands appear at around 848 and 858 nm, which suggested the formation of Pu(VI) hydrolysis species. The absorption band position of 848 nm suggested the occurrence of polynuclear hydrolysis species like  $(\text{PuO}_2)_2(\text{OH})_2^{2+}$  (e.g. Reilly and Neu 2006). Those species are formed in the millimolar Pu(VI) concentration range. Whereas at lower Pu(VI) concentrations below  $10^{-4}$  M the monomeric species are dominant. The absorption band

detected at 848 nm is most likely the sum signal from  $\text{PuO}_2\text{OH}^+$  and  $(\text{PuO}_2)_2(\text{OH})_2^{2+}$ . The shoulder detected at 858 nm might indicate the influence of  $\text{PuO}_2(\text{OH})_2$  (aq) which is characterized by an absorption band at 850.3 nm (e.g. Cho et al. 2010). At pH 6.1 and based on the results coming from the absorption spectra the cells are interacting mainly with Pu(VI)-hydrolysis species. The signal of  $\text{PuO}_2^{2+}$  decreased much faster than the sum signal of the Pu(VI)-hydroxo species (cf. Figure 4 a left). This could mean that  $\text{PuO}_2^{2+}$  showed a higher affinity to sorb on the bacterial surface. At incubation times > 49 hours no safe prediction can be made regarding the Pu(VI) amount in the supernatant. The decrease of the Pu(VI) signal is much faster than in the blank samples (cf. Figure 4 a right). As a function of the incubation time we detected an increase of the typical absorption band of Pu(V) at 569 nm (cf. Figure 4 b).

**Biomass.** The summary of all extraction data observed in the electron-donor free experiments with *Sporomusa* sp. showed scattered concentration data of the individual plutonium oxidation states (cf. Figure S5a). No differences of the time-dependent Pu oxidation state distributions were detected as a function of  $[\text{Pu}]_{\text{initial}}$ . The exponential decay functions shown in Figure S5a were only used to estimate the average amount of the individual Pu oxidation states. No defined time dependencies of the Pu oxidation states could be seen from the measurements (cf. Figure S5a). Therefore, the steady state concentrations of the major Pu oxidation states identified on the biomass are depicted in Figure 3 b. At pH 6.1 the major Pu oxidation state was Pu(IV)-polymers with an average amount of  $42 \pm 4$  %. Also at pH 4 the tetravalent Pu dominates (37 % Pu(IV) and 25 % Pu(IV)-polymers). The Pu(III) average amount of 27 % at pH 6.1 is clearly higher than found in the blanks and supernatants. At both pH values the fraction of Pu which was not accessible by the extraction technique amounted to 30 %. This plutonium could be masked for instance by an uptake in biomass. And can be also correlated with the amount of irreversibly bound Pu (*Sporomusa* sp.: 40 - 60 %).

## Time-dependent Pu oxidation state distributions – with electron donor

**The blank.** Compared to the pyruvate-free system (cf. supplementary material Figure S6 a and b) a more complex Pu redox-chemistry was observed. The observed changes in the individual Pu oxidation states are triggered by both natural occurring reduction/oxidation reactions (as depicted in Figure S4 a and b) and reduction processes promoted by Na-pyruvate (cf. supplementary material Figure S6 a and b). At the beginning at pH 6.1, the major oxidation states (complexed with pyruvate) interacting with the

biomass are Pu(V) with 31 %, Pu(IV) with 22 %, and Pu(IV)-polymers with 23 %. At the beginning at pH 4, the major oxidation states (complexed with pyruvate) interacting with the biomass are Pu(IV) with 39 %, Pu(V) with 20 %, and Pu(IV)-polymers with 24 %. At pH 6.1 within the first 1.2 h the amount of Pu(VI) decreased from 61 % to about 4 %. At pH 4 after 2 h almost no Pu(VI) could be detected. At both pH values simultaneously Pu(V) and Pu(IV) increased to about 31 % (22 % at pH 4) and 22 % (45 % at pH 4), respectively. At pH of 6.1, we observed also an increase of Pu(IV)-polymers from 19 % in the beginning to about 34 % at the end of the experiment. This could be explained by a transfer of the formed Pu(IV) into Pu(IV)-polymers at this pH. At pH 4 the Pu(IV)-polymer fraction remained constant at  $27 \pm 3$  %. Pu(V) was abiotically reduced to Pu(IV) due to the presence of pyruvate. Later on ( $t \geq 144$  h) an increase of Pu(III) in combination with an decrease of Pu(IV) at pH 6.1 was observed (cf. Figure S6 b). This might indicate a further reduction of Pu(IV) forming Pu(III). Hence, to model the Pu(IV) behavior at pH 6 the data were split into two time ranges. First, there was an exponential growth of Pu(IV) followed by an exponential decrease. In contrast at pH 4, there was an exponential growth of the Pu(IV) fraction with a steady state concentration of 70 % (major difference between both pH values). At pH 6.1 an exponential growth of Pu(III) with an equilibrium concentration of 55 % was calculated. Whereas at pH 4 for a very low Pu(III) equilibrium concentration of ca. 0.1 % was found.

*The supernatant.* At pH 6.1 a similar behavior of dominating Pu oxidation states could be observed as found in the blanks (cf. Figure 3 c and S6 d). However, due to cell induced effects the formation of Pu(III) as the major oxidation state is 68 times faster than in blank samples. The decrease of Pu(IV) in the supernatant is 9 times faster than in the blanks. The decrease of Pu(V) is 35 times faster than in the blank samples. Under steady state conditions similar concentrations of Pu(III) (~50 %), Pu(IV) (~15 %), and Pu(V) (~1 %) were measured in blanks and the *Sporomusa* sp. supernatants. In contrast to pH 6.1 at pH 4 in the *Sporomusa* sp. system a clear enrichment of Pu(IV) was observed (cf. Figure S6 c). At pH 4 the main difference compared to the blanks due to cell mediated processes was a faster increase of Pu(IV) (33 times), and slightly lower concentrations of Pu(IV)-polymers (23.2 %).

*The biomass.* At pH 6.1 there was a clear enrichment of Pu(III) in the biomass in the presence of 10 mM Na-pyruvate (Figure 3 d and Figure S5 b), whereas Pu(IV)-polymers associated on biomass dominated in the sample without additional electron donor (Figure 3 b). A steady state concentration of  $70 \pm 4$  % for Pu(III) was observed. This amount is three times higher than in the electron donor free system. In the presence of Na-pyruvate, the Pu(IV)-polymer concentration in the biomass yielded lower

steady state concentrations than in the electron donor free experiments. Therefore, we assume a transfer of Pu(IV)-polymers into Pu(III) promoted by pyruvate and by reducing electrochemical zones provided by the bacterial cell membrane (e.g. Neu et al. 2005). From the pyruvate concentration-dependent experiments one can conclude that 0.011 g/L pyruvate has a similar influence on the Pu redox chemistry as 0.33 g/L *Sporomusa* sp. MT-2.99 cells. The decrease of the Pu(IV)-polymer amount is approximately 4 times faster at pH 6.1 compared to pH 4. The equilibrium amount is with 23.5 % equal for both pH values. The main difference (as also observed in the blank and the supernatants) is an enrichment of Pu(IV) on the biomass at pH 4 (cf. Figure 3 d and S6 e), whereas Pu(III) was enriched at pH 6.1.

## Discussions

*0.1 M NaClO<sub>4</sub> no donor.* A very fast decrease of Pu(VI) in solution in the presence of cells was observed (cf. Figure S4 C and D; Figure 3 a). This process is connected with a fast increase of Pu(V). However, this Pu(V) was not observed on the cells. There must be a fast reduction (cell promoted because it was faster than in the blanks) forming Pu(V) in the vicinity of the cells or at the cell surface after a fast bioassociation of Pu(VI) (cf. Figure 5). Under steady state conditions the equilibrium concentration of Pu(VI) was 4.1  $\mu$ M (0.04  $\mu$ M at pH 6.1) in the supernatants not interacting with the cells. A clear enrichment of Pu(IV)-polymers on the biomass could be seen (cf. Table 1) especially at pH 6.1. Here, the Pu(IV)-polymer concentration is higher on the biomass in comparison to blanks and supernatants. The cells could induce a transformation process forming Pu(IV)-polymers from the sorbed Pu(IV). In a first very fast step there was most likely an association of Pu(VI) and Pu(IV)-polymers at the cell envelope followed by a reduction forming Pu(V). This process is ca. 48 times faster than in blank samples. Ohnuki et al. reported also the reduction of Pu(VI) to Pu(V) in their experiments with *B. subtilis* with and without kaolinite clay (Ohnuki et al. 2009). The observed second step the reduction of Pu(V) to Pu(IV) was not observed in our experiments. Pu(V) identified in the supernatants can disproportionate in aqueous solution forming Pu(IV) and Pu(VI) (e.g. Nitsche et al. 1988). Pu(VI) was found in the supernatants. Whereas Pu(IV) was associated on the biomass. Part of this Pu(IV) could be further reduced to Pu(III). At pH 6.1 we observed higher amounts of Pu(III) on the biomass compared with pH 4. Simultaneously lower values of Pu(IV) were detected. Hence, there was a stronger tendency of a transformation of the bioassociated Pu(IV) forming Pu(III). Here dead biomass might act as an electron donor. However, the

mechanism of this Pu(IV) reduction is not clear at the moment.

*10 mM Na-pyruvate pH 4.* The time-dependent Pu oxidation state distribution is driven by the reducing properties of Na-pyruvate. Under steady state conditions (cf. Table 2) the concentration of Pu(IV) in blanks was 40  $\mu$ M. Approximately half of it, ca. 20  $\mu$ M, was found in the supernatant and on the biomass each. The formation of Pu(IV) in the supernatant was 68 times faster than in blanks. At the beginning there was a biosorption of Pu(IV)-polymers on the biomass. This Pu(IV)-polymer fraction decreased with time and was accompanied by an increase of Pu(IV). This Pu(IV) concentration can be a result of the biosorption of Pu(IV) from the supernatant and/or of a biotransformation of Pu(IV)-polymers into Pu(IV) in the biomass (cf. Figure 5). It is difficult to postulate a direct bio-reduction of Pu(VI) forming Pu(IV) by *Sporomusa* sp. cells. Interestingly, no further reduction of Pu(IV) to Pu(III) was observed.

*10 mM Na-pyruvate pH 6.1.* At incubation times within 0 and 200 h in the blanks mainly Pu(IV) and Pu(IV)-polymers were detected (cf. Figure S6 b). However, on the biomass the major Pu oxidation states were always Pu(III) in addition to Pu(IV)-polymers. The formation of Pu(III) is 68 times faster in the supernatants and 2 times faster on the cells compared with the dependencies in the blanks. First a biosorption of Pu(IV) (and Pu(IV)-polymers) could be the initial step followed by a bio-reduction forming Pu(III). In addition a biotransformation of Pu(IV)-polymers into Pu(III) seems possible. The majority of Pu(III) was found on the biomass (cf. Figure 5). One explanation would be a cell catalyzed bio-reduction process of Pu(IV) and Pu(IV)-polymers in the presence of 10 mM Na-pyruvate at pH 6.1. The potential of microbes to reduce Pu(IV) to Pu(III) in the presence of electron donors was reported in (e.g. Boukhalfe et al. 2007; Renshaw et al. 2009).

## Conclusions

In this study, the interaction of Pu with the bacterium, *Sporomusa* sp. MT-2.99, isolated from Mont Terri Opalinus Clay, was investigated in 0.1 M NaClO<sub>4</sub> as a function of the initial Pu concentration, the pH, and with and without the addition of Na-pyruvate as an electron donor. In the electron donor containing system faster kinetics were found. The isolate displayed a strong pH-dependent affinity for Pu. Using the Langmuir model the maximal Pu loading at pH 6.1 on *Sporomusa* sp.,  $230 \pm 14$  mg Pu / g<sub>dry weight</sub>, was calculated. The maximal loadings are high compared to literature values (e.g. Panak and

Nitsche 2001; Moll et al. 2006). Hence, *Sporomusa* sp. cells were efficient in removing Pu from the surrounding solution. In the presence *Sporomusa* sp. cells a change in the Pu oxidation state distributions was discovered in comparison to the abiotic controls (cf. Figure 5). In the absence of added organics there was a fast increase of Pu(V) in the cell suspensions. On the biomass an enrichment of Pu(IV)-polymers independent of  $[Pu]_{\text{initial}}$  and pH was observed. The dominance of Pu(V) in the cell suspensions could be explained by the decrease of  $E_h$ , a possible release of complexing agents by the cells and by reducing properties of the cells itself. For example a release of such agents was concluded for suspensions of the Mont Terri Opalinus Clay isolate *Paenibacillus* sp. in the presence of U(VI) (Lütke et al. 2013). The role of residual organics present in biologically active systems to reduce Pu(VI) species to Pu(V) species at near-neutral pH was pointed out in Reed et al. 2007. The predominance of Pu(V) might indicate biologically active systems at least in the starting phase of our experiments. In the presence of 10 mM Na-pyruvate the Pu oxidation state distribution was pH-dependent. Under steady state conditions the redox potential was measured to be ca. 480 mV in abiotic controls and cell suspensions at pH 4. Using Figure 1 as an approximate Pu(IV) should be the dominant oxidation state. Approximately 50 % remains in solution of the cell suspensions and 50 % was associated with the cells. The influence of the cells is pronounced in a faster enrichment of Pu(IV). At pH 6.1 again under steady state conditions the redox potential in abiotic controls and cell suspensions was measured to be 190 mV. Using Figure 1 as an approximate Pu(III) should be the dominant oxidation state. In agreement with the observations: 76 % of Pu(III) was found on the biomass and 24 % in the supernatant. Therefore, the cells induced a faster formation of Pu(III) compared to the abiotic controls.

To conclude, a moderate to strong impact of *Sporomusa* sp. cells on the Pu speciation was observed (cf. Figure 5). The presented results contribute to a better mechanistic understanding of Pu biogeochemistry in the presence of host rock indigenous bacterial cells.

## Acknowledgements

The authors thank the BMWi for financial support (contract no.: 02E10618 and 02E10971), Velina Bachvarova and Sonja Selenska-Pobell for isolation of the bacterial strain, Monika Dudek for strain cultivation and the BGR for providing the clay samples. Thanks to Laura Lütke for valuable help in strain characterization and many fruitful discussions as well as Susanne Sachs and Katja Schmeide for help in preparing the Pu-242 stock solution.

## References

- Atkins PW (1998) Physical Chemistry. Oxford University Press, Oxford, UK.
- Bachvarova V, Geissler A, Selenska-Pobell S (2009) Bacterial isolates cultured under anaerobic conditions from an opalinus clay sample from the Mont Terri Rock laboratory. FZD-530 FZD-IRC Annual Report, 18.
- Bethke CM (2008) "Geochemical and Biogeochemical Reaction Modeling" 2<sup>nd</sup> Ed., Cambridge University Press, 543 pp.
- Boukhalfa H, Icopini GA, Reilly SD, Neu MP (2007) Plutonium(IV) reduction by the metal-reducing bacteria *Geobacter metallireducens* GS-15 and *Shewanella oneidensis* MR-1. Appl Environ Microbiol 73:5897–5903.
- Brookshaw DR, Patrick RAD, Lloyd JR, Vaughan DJ (2012) Microbial effects on mineral-radionuclide interactions and radionuclide solid-phase capture processes. Mineral Mag 76:777–806.
- Cho H-R, Jung EC, Park KK, Kim WH, Song K, Yun J-I (2010) Spectroscopic study on the mononuclear hydrolysis species of Pu(VI) under oxidation conditions. Radiochim Acta 98:765–770.
- Francis AJ (2007) Microbial mobilization and immobilization of plutonium. J Alloys Compd 444-445:500-505.
- Francis AJ, Dodge CJ, Gillow, JB (2008) Reductive dissolution of Pu(IV) by *Clostridium* sp. under anaerobic conditions. Environ Sci Technol 42:2355-2360.
- Francis AJ, Dodge CJ (2015) Microbial mobilization of plutonium and other actinides from contaminated soil. J Environ Radioact 150:277-285.
- Guillaumont R, Fanghänel T, Fuger J, Grenthe I, Neck V, Palmer DA, Rand MH (2003) Chemical Thermodynamics Series Volume 5: Update on the Chemical Thermodynamics of Uranium, Neptunium, Plutonium, Americium and Technetium, Elsevier, Amsterdam, 960 pp.
- Icopini GA, Lack JG, Hersman LE, Neu MP, Boukhalfa H (2009) Plutonium(V/VI) reduction by the metal-reducing bacteria *Geobacter metallireducens* GS-15 and *Shewanella oneidensis* MR-1. Appl Environ Microbiol 75:3641–3647.
- Joseph C, Van Loon LR, Jakob A, Steudtner R, Schmeide K, Sachs S, Bernhard (2013) Diffusion of U(VI) in Opalinus Clay: Influence of temperature and humic acid. Geochim Cosmochim Acta 75:352–367.

502 Keller C (1971) The Chemistry of the Transuranium Elements, Volume 3, Verlag Chemie GmbH,  
 503 Weinheim, Germany.

504 Kersting AB (2013) Plutonium transport in the environment. *Inorg Chem* 52:3533-3546.

505 Klimmek S (2003) Charakterisierung der Biosorption von Schwermetallen an Algen. PhD thesis,  
 506 Technische Universität Berlin, Berlin, Germany.

507 Kimber RL, Boothman C, Purdie P, Livens FR, Lloyd JR (2012) Biogeochemical behavior of plutonium  
 508 during anoxic biostimulation of contaminated sediments. *Mineral Mag* 76:567-578.

509 Kümmel R, Worch E (1990) Adsorption aus wässrigen Lösungen. Dt. Verl. für Grundstoffindustrie:  
 510 Leipzig, Germany.

511 Lemire RJ, Fuger J, Nitsche H, Potter P, Rand MH, Rydberg J, Spahiu K, Sullivan JC, Ullman W,  
 512 Vitorge P, Wanner H (2001) Chemical Thermodynamics Series Volume 4: Chemical  
 513 Thermodynamics of Neptunium and Plutonium, Elsevier, Amsterdam, 870 pp.

514 Lloyd JR, Gadd GM (2011) The Geomicrobiology of Radionuclides. *Geomicrobiol J* 28:383–386.

515 Lukšienė B, Druteikienė R, Pečiulytė D, Baltrūnas D, Remeikis V, Paškevičius A (2012) Effect of  
 516 microorganisms on the plutonium oxidation states. *Appl Radiat Isot* 70:442-449.

517 Lütke L, Moll H, Bachvarova V, Selenska-Pobell S, Bernhard G (2013) The U(VI) speciation influenced  
 518 by a novel *Paenibacillus* isolate from Mont Terri Opalinus clay. *Dalton Trans* 42:6979-6988.

519 Moll H, Merroun ML, Hennig Ch, Rossberg A, Selenska-Pobell S, Bernhard G (2006) The interaction of  
 520 *Desulfovibrio äspöensis* DSM 10631<sup>T</sup> with plutonium. *Radiochim Acta* 94:815-824.

521 Moll H, Lütke L, Bachvarova V, Cherkouk A, Selenska-Pobell S, Bernhard G (2014) Interactions of the  
 522 Mont Terri Opalinus Clay Isolate *Sporomusa* sp. MT-2.99 with Curium(III) and Europium(III).  
 523 *Geomicrobiol J* 31:682-696.

524 Neu MP, Icopini GA, Boukhalfa H (2005) Plutonium speciation affected by environmental bacteria.  
 525 *Radiochim Acta* 93:705–714.

526 Neu MP, Boukhalfa H, Merroun ML (2010) Biomineralization and biotransformations of actinide  
 527 materials. *MRS Bulletin* 35:849–857.

528 Nitsche H, Lee SC, Gatti RC (1988) Determination of plutonium oxidation states at trace levels pertinent  
 529 to nuclear waste disposal. *J Radioanal Nucl Chem* 124:171–185.

530 Nitsche H, Roberts K, Xi R, Prussin T, Becraft K, Mahamid IA, Silber HB, Carpenter SA, Gatti RC  
 531 (1994) Long term plutonium solubility and speciation studies in a synthetic brine. *Radiochim Acta*

532 66/67:3–8.

533 Newsome L, Morris K, Lloyd JR (2014) The biogeochemistry and bioremediation of uranium and other  
 534 priority radionuclides. *Chem Geol* 363:164-184.

535 Ockenden DW, Welch GA (1956) The Preparation and Properties of Some Plutonium Compounds. Part  
 536 V.\* Colloidal Quadrivalent Plutonium. *J Chem Soc* :3358–3363.

537 Ohnuki T, Yoshida T, Ozaki T, Kozai N, Sakamoto F, Nankawa T, Suzuki Y, Francis AJ (2009)  
 538 Modeling of the interaction of Pu(VI) with the mixture of microorganism and clay. *J Nucl Sci Technol*  
 539 46:55–59.

540 Ohnuki T, Kozai N, Sakamoto F, Ozaki T, Nankawa T, Suzuki Y, Francis AJ (2010) Association of  
 541 actinides with microorganisms and clay: Implications for radionuclide migration from waste-  
 542 repository sites. *Geomicrobiol J* 27:225–230.

543 Panak PJ, Nitsche H (2001) Interaction of aerobic soil bacteria with plutonium(VI). *Radiochim Acta*  
 544 89:499–504.

545 Poulain S, Sergeant C, Simonoff M, Le Marrec C, Altmann S (2008) Microbial investigations in opalinus  
 546 clay, an argillaceous formation under evaluation as a potential host rock for a radioactive waste  
 547 repository. *Geomicrobiol J* 25:240-249.

548 Reed DT, Pepper SE, Richmann MK, Smith G, Deo R, Rittmann BE (2007) Subsurface bio-mediated  
 549 reduction of higher-valent uranium and plutonium. *J Alloys Compd* 444-445:376–382.

550 Reilly SD, Neu MP (2006) Pu(VI) Hydrolysis: Further Evidence for a Dimeric Plutonyl Hydroxide and  
 551 Contrasts with U(VI) Chemistry. *Inorg Chem* 45:1839–1846.

552 Renshaw JC, Law N, Geissler A, Livens FR, Lloyd JR (2009) Impact of the Fe(III)-reducing bacteria  
 553 *Geobacter sulfurreducens* and *Shewanella oneidensis* on the speciation of plutonium.  
 554 *Biogeochemistry* 94:191–196.

555 Roh C, Kang C, Lloyd JR (2015) Microbial bioremediation processes for radioactive waste. *Korean J*  
 556 *Chem Eng* 32:1720-1726 and references therein.

557 Swanson JS, Reed DT, Ams DA, Norden D, Simmons KA (2012) Status report on the microbial  
 558 characterization of halite and groundwater samples from the WIPP, Los Alamos National Laboratory,  
 559 p. 1.

560 Thury M, Bossart P (1999) The Mont Terri Rock Laboratory, a new international research project in a  
 561 Mesozoic shale formation, in Switzerland. *Eng Geol* 52:347-359.

562 Wilson RE, Hu Y-J, Nitsche H (2005) Detection and quantification of Pu(III, IV, V, and VI) using a 1.0-  
563 meter liquid core wave guide. *Radiochim Acta* 93:203-206.

564 Wouters K, Moors H, Boven P, Leys N (2013) Evidence and characteristics of a diverse and  
565 metabolically active microbial community in deep subsurface clay borehole water. *FEMS Microb*  
566 *Ecol* 86:458–473.

567

568

## Tables

**Table 1** Quantification of the different Pu oxidation states in the *Sporomusa* sp. system determined by solvent extractions in combination with LSC in the 0.1 M NaClO<sub>4</sub> experiments under steady state conditions ([Pu]<sub>initial</sub> 59 ± 4 μM).

	pH 4			pH 6		
	Blank	Supernatant	Biomass	Blank	Supernatant	Biomass
Pu(IV) μM	-	-	10.7	0.4	-	5.4
Pu(VI) μM	22.5	4.1	-	2.5	0.04	-
Pu(III) μM	-	-	5.3	3.7	-	16.7
Pu(V) μM	17.3	14.1	-	47.1	1.76	-
Pu(IV)-Polymers μM	10.9	3.9	8.6	7.75	0.11	25.2
[Pu] μM	55.7	23.1	32.6	62.0	2.0	60
	100 %	41.5 %	58.5 %	100 %	3.2 %	96.8 %

**Table 2** Quantification of the different Pu oxidation states in the *Sporomusa* sp. system determined by solvent extractions in combination with LSC in the presence of 10 mM Na-pyruvate under steady state conditions ([Pu]<sub>initial</sub> 57 ± 1 μM, 0.1 M NaClO<sub>4</sub>).

	pH 4			pH 6		
	Blank	Supernatant	Biomass	Blank	Supernatant	Biomass
Pu(IV) μM	40.1	20.2	18.3	10.2	2.3	3.8
Pu(VI) μM	-	-	-	-	-	-
Pu(III) μM	0.06	1.83	0.94	31.1	8.01	26.0
Pu(V) μM	-	-	-	-	0.02	-
Pu(IV)-Polymers μM	16.4	6.54	6.76	15.9	6.0	8.9
[Pu] μM	57.6	28.2	29.4	56.5	17.8	38.7
	100%	48.9%	51.0%	100%	31.5%	68.5%

## Figure legends

**Fig. 1** Eh – pH diagram of Pu calculated for a 0.1 M NaClO<sub>4</sub> solution with 180 μM Pu in the absence of CO<sub>2</sub> at 25 °C. The diagram was constructed using geochemical speciation “Geochemist’s Workbench”<sup>®</sup> 11.0.3 (Bethke 2008) with the NEA Thermochemical Database (Lemire et al. 2001; Guillaumont et al. 2003). The diagram includes the measured Eh and pH values from selected experiments at pH 3, 4, 6.1, and 7 (blanks and corresponding cell suspensions).

**Fig. 2** a and b: Decrease of [<sup>242</sup>Pu] in solution at [<sup>242</sup>Pu]<sub>initial</sub>: 188 ± 3 μM in 0.1 M NaClO<sub>4</sub> at pH 4 and 6.1 after contact with 0.34 g<sub>dry weight</sub>/L of *Sporomusa* sp. MT-2.99. The red line represents the best fit of the experimental data. c: Langmuir isotherms obtained in the *Sporomusa* sp. system at pH 4 and 6.1 including the Langmuir absorption isotherm data (a<sub>m</sub> maximal Pu loading, b Langmuir constant, R<sup>2</sup> goodness of fit).

**Fig. 3** Average <sup>242</sup>Pu oxidation state distributions determined by solvent extraction in 0.1 M NaClO<sub>4</sub> without electron donor a) in the supernatant ([dry biomass] 0.34 g/L) at pH 6.1 and b) in the biomass ([dry biomass] 0.34 g/L at pH 4 and 6.1 as well as in the presence of 10 mM Na-pyruvate: c) in the supernatant ([dry biomass] 0.34 g/L at pH 6.1) and d) in the biomass at pH 4 and pH 6.1.

**Fig. 4** Absorption spectra of Pu ([<sup>242</sup>Pu]<sub>initial</sub> = 450 ± 20 μM) in 0.1 M NaClO<sub>4</sub> at pH 6.1: a) wavelength range of Pu(VI): the supernatants after different contact times with 0.34 g<sub>dry weight</sub>/L of *Sporomusa* sp. after separating the cells by centrifugation (left) and the blanks (right); b) wavelength range of Pu(V): the supernatants.

**Fig. 5** Illustration of the main processes describing the complex interaction of Pu with *Sporomusa* sp. MT-2.99 cells.

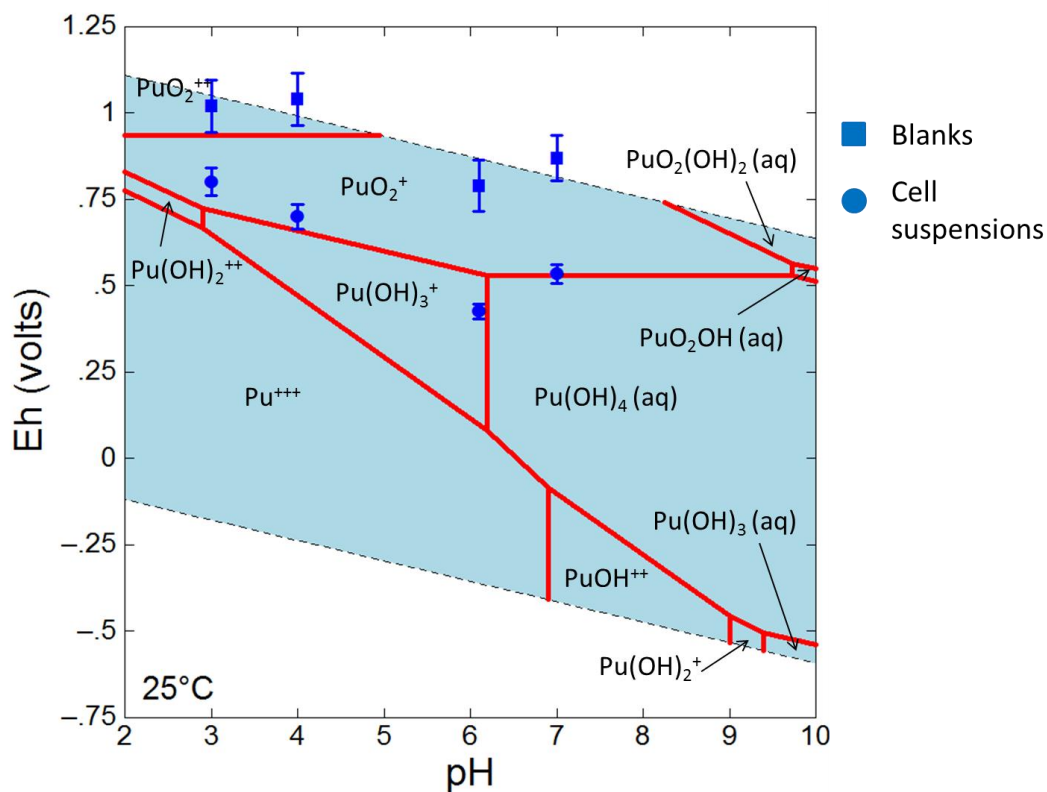


**Fig. 1** Eh – pH diagram of Pu calculated for a 0.1 M  $\text{NaClO}_4$  solution with 180  $\mu\text{M}$  Pu in the absence of  $\text{CO}_2$  at 25 °C. The diagram was constructed using geochemical speciation “Geochemist’s Workbench”<sup>®</sup> 11.0.3 (Bethke 2008) with the NEA Thermochemical Database (Lemire et al. 2001; Guillaumont et al. 2003). The diagram includes the measured Eh and pH values from selected experiments at pH 3, 4, 6.1, and 7 (blanks and corresponding cell suspensions).

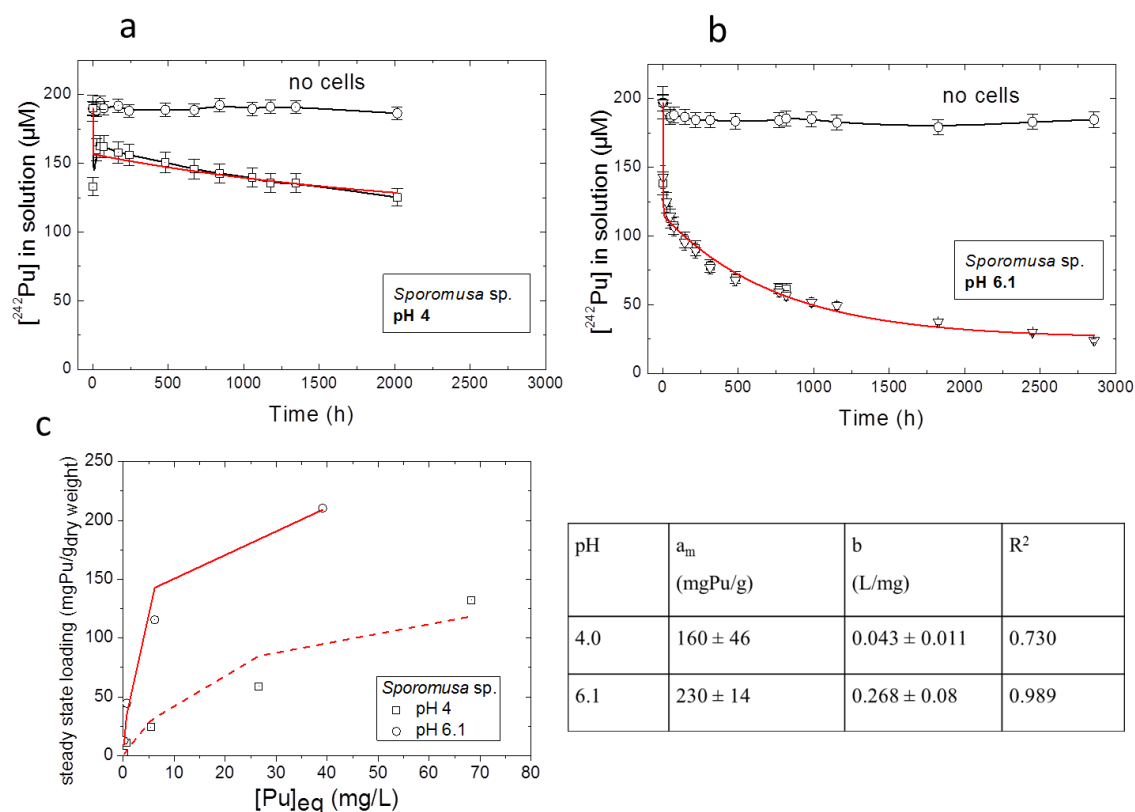
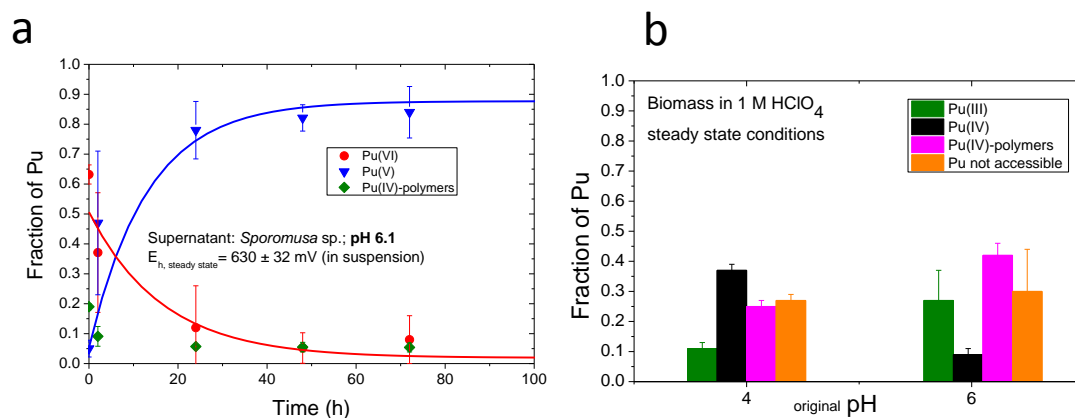


**Fig. 2** a and b: Decrease of  $^{242}\text{Pu}$  in solution at  $^{242}\text{Pu}_{\text{initial}}$ :  $188 \pm 3 \mu\text{M}$  in 0.1 M  $\text{NaClO}_4$  at pH 4 and 6.1 after contact with 0.34 g<sub>dry weight</sub>/L of *Sporomusa* sp. MT-2.99. The red line represents the best fit of the experimental data. c: Langmuir isotherms obtained in the *Sporomusa* sp. system at pH 4 and 6.1 including the Langmuir absorption isotherm data ( $a_m$  maximal Pu loading,  $b$  Langmuir constant,  $R^2$  goodness of fit).

Without electron donor;  $[^{242}\text{Pu}]_{\text{initial}}: 450 \pm 20 \mu\text{M}$



With electron donor;  $[^{242}\text{Pu}]_{\text{initial}}: 57 \pm 2 \mu\text{M}$

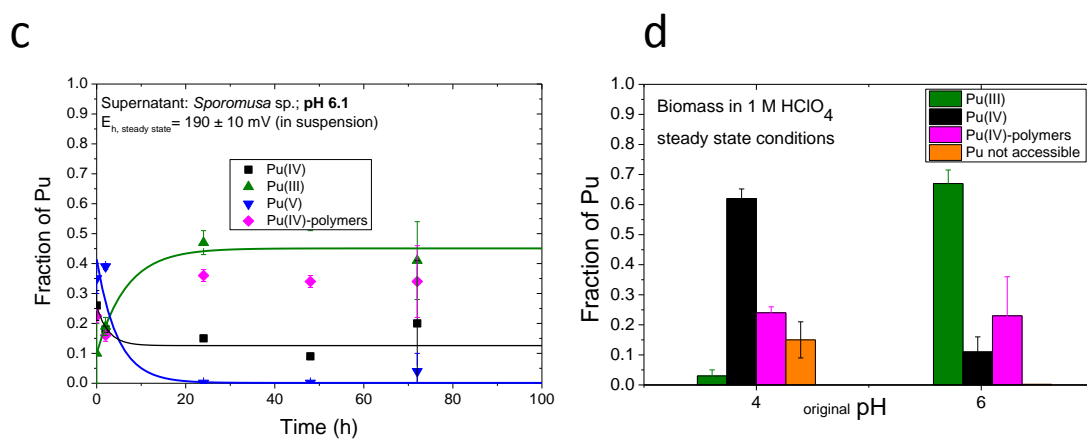


**Fig. 3** Average  $^{242}\text{Pu}$  oxidation state distributions determined by solvent extraction in 0.1 M NaClO<sub>4</sub> without electron donor a) in the supernatant ([dry biomass] 0.34 g/L) at pH 6.1 and b) in the biomass ([dry biomass] 0.34 g/L at pH 4 and 6.1 as well as in the presence of 10 mM Na-pyruvate: c) in the supernatant ([dry biomass] 0.34 g/L at pH 6.1) and d) in the biomass at pH 4 and pH 6.1.

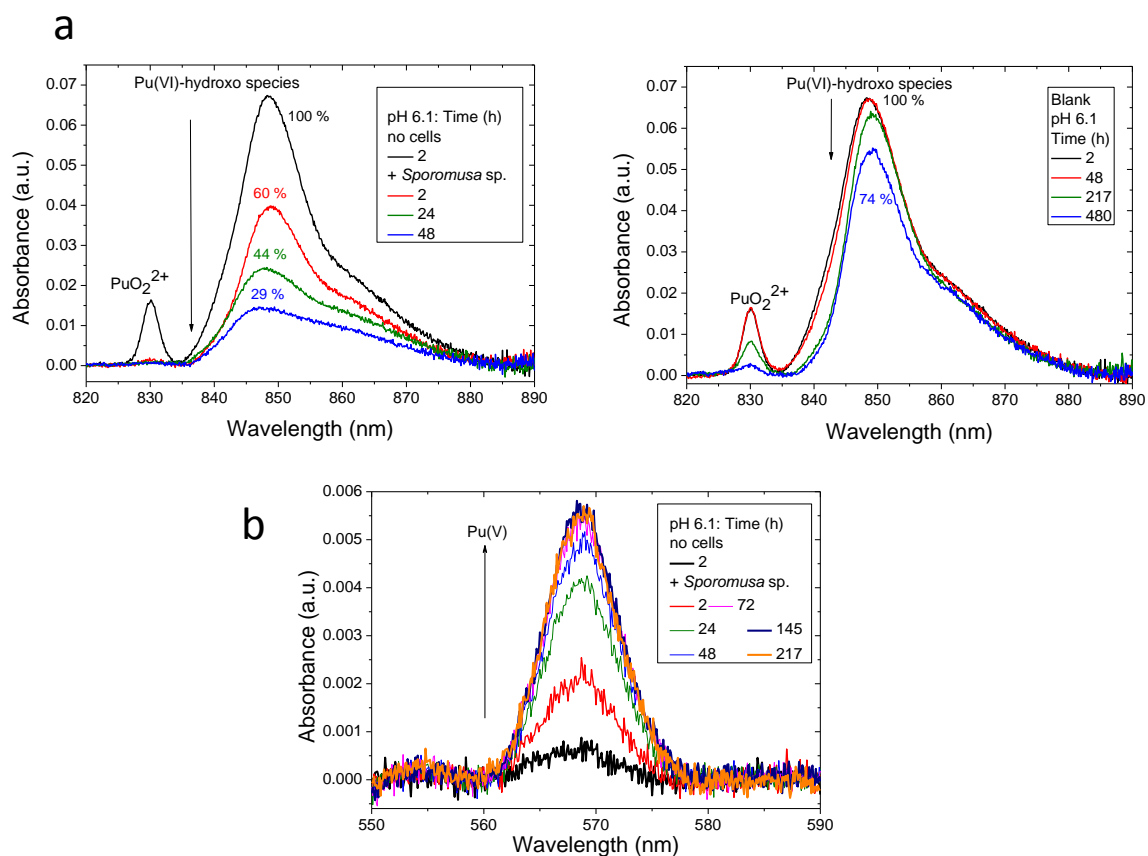


**Fig. 4** Absorption spectra of Pu ( $[\text{}^{242}\text{Pu}]_{\text{initial}} = 450 \pm 20 \mu\text{M}$ ) in 0.1 M  $\text{NaClO}_4$  at pH 6.1: a) wavelength range of Pu(VI): the supernatants after different contact times with 0.34 g<sub>dry weight</sub>/L of *Sporomusa* sp. after separating the cells by centrifugation (left) and the blanks (right); b) wavelength range of Pu(V): the supernatants.

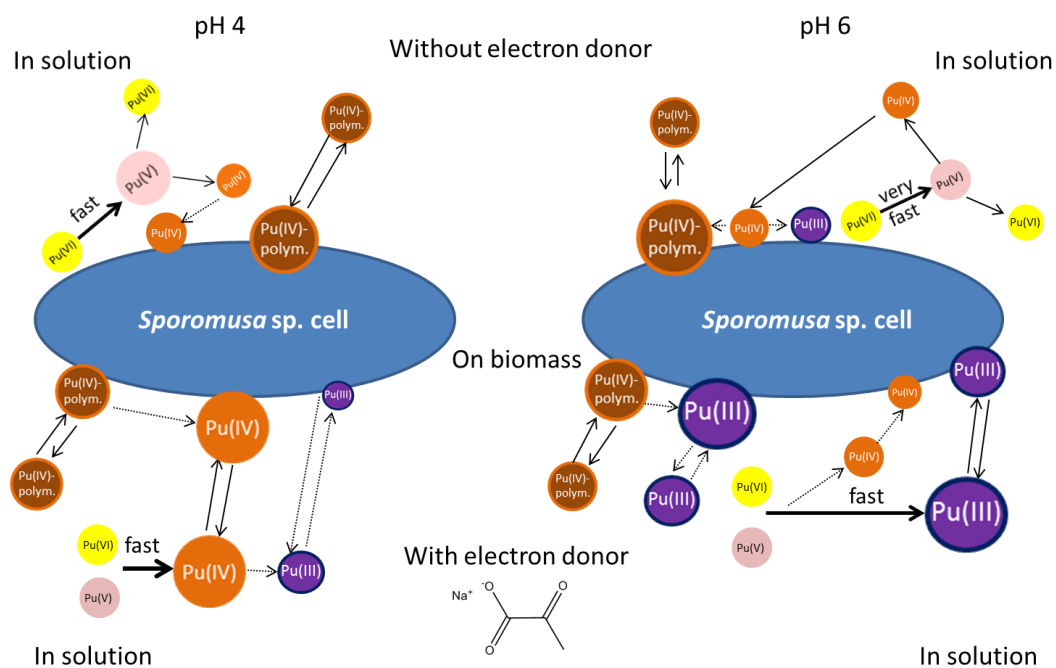


**Fig. 5** Illustration of the main processes describing the complex interaction of Pu with *Sporomusa* sp. MT-2.99 cells.